DEVELOPMENT OF NOVEL SHEAR CONNECTORS FOR COLD-FORMED STEEL CONCRETE COMPOSITE BEAMS

M. Divya[1], R. Senthil Kumar[1], Prince George[1], P. Jayabalan[1], Konstantinos Daniel Tsavdaridis[2], A. Bahurudeen[3]

[1]Department of Civil Engineering, National Institute of Technology Tiruchirappalli, Tiruchirappalli., Tamil Nadu, India.

[2]Department of Engineering, School of Science & Technology, City, University of London, Northampton Square, EC1V 0HB, London, UK.

[3] Department of Civil Engineering, Birla Institute of Technology and Science, Hyderabad campus, Hyderabad.

ABSTRACT

The usage of cold-formed steel members as a primary structural element has increased drastically, paving the way for developing cold-formed steel-concrete composite members. The shear connectors are key elements to provide the composite action between steel and concrete. The research on suitable shear connectors for cold-formed steel-concrete composite members has been widely investigated. This study evaluates the behavior of three novel shear connectors. The proposed shear connectors were anchored without welding, making them suitable for light gauge sections by reducing the formation of residual stresses and geometrical imperfections. The first two shear connectors (trapezoidal and hexagonal) were anchored using self-tapping screws. The third one, the prefabricated shear connector, was incorporated by adopting suitable modifications in the beam without external connecting arrangements. The behaviour of connectors was assessed by conducting push-out tests as per Eurocode 4. The shear capacity, characteristic slip, initial stiffness, load-slip relationship, ductility, and energy absorption capacity of the connectors were analysed and presented. It is observed that the prefabricated shear connector has recorded the highest shear capacity and energy absorbing capacity among the proposed connectors.

Notation				
f_y	Yield strength	L_c	Length of connector
f_u	Ultimate strength	Φ	Diameter of screws
E_s	Modulus of Elasticity of steel	C_C	Capacity of Connection
E_c	Modulus of Elasticity of concrete	C_{PS}	Capacity Per Screw
y'	Elongation of the specimen	δ_{rk}	Characteristic slip ($0.9\ \delta_u$)
f_{cu}	Cube compressive strength	LVDT	Linear Variable Displacement Transducers
f_{cy}	Cylinder Compressive Strength	TC	Trapezoidal shear Connector
σ	Standard deviation	HC	Hexagonal shear Connector
cov	Coefficient of Variation	PF	Prefabricated Shear Connector
P_u	Ultimate load carrying capacity of the connector	STC	Stud Connector for hot-rolled composite beam

P_{rk}	Characteristic resistance of the connector	CH	Channel connector for Hot-rolled composite beam
δ_u	Slip of the connector at maximum value of P_{rk}	SC	Single Channel cold-formed steel connector
δ_y	yield slip at the minimum value of P_{rk}	DC	Double Channel cold-formed steel connector
FP	Flat Plate.	ST	Self-Tapping screw shear connector
W_c	Weight of a connector	DAQ	Data Acquisition system
EA	Energy Absorption capacity.	UTM	Universal Testing Machine
LRFD	Load and Resistance Factor Design	DF	Ductility Factor

1. INTRODUCTION

Over the past few decades, there has been a substantial rise in the industrial demand for lightweight flooring systems and sustainable green constructions. Cold-formed steel (CFS) members are preferred over other hot-rolled structural members since they have a tremendous strength-to-weight ratio, ease to produce, assemble on the site and resource-friendly. The CFS members were primarily used for mezzanine floors, but they are now commonly adopted for constructing residential and commercial buildings, especially for low-rise structures [1]. It has become a popular choice in the construction industry and these sections are often used as beams, columns, wall panels, and floor members. The CFS sections are generally manufactured by two methods: press braking or forging and roll forming. The mechanical properties of CFS and hot-rolled sections differ as they undergo distinct manufacturing methods. The CFS section shows increased yield strength at the corner regions up to 80% without disturbing the ultimate strength of the material and accompanied by 27% [2] reduced ductility and disappearance of yield plateau of the virgin material [3]. The light gauge cold-formed steel sections are susceptible to various forms of instabilities such as local, distortional, and lateral torsional buckling [4]. The buckling modes depend on the cross-sectional dimensions, effective length and boundary conditions of the sections. The local buckling shows the rotation of the individual plate elements forming the cross section by preserving the internal nodal lines (internal edges) of the section and it is also accompanied by repeated short wavelengths **(Figure 1)**, the distortional buckling is characterized by deformation of the internal edges by both rotation and translation and its wavelength is intermediate between local and lateral torsional buckling **(Figure 2)**. The lateral torsional buckling shows the translation and rotation of the whole section of the beam along its length as shown in **Figure 3.** The Buckling modes happen when the CFS section experience compressive forces, and they can be prevented by exposing the element solely to tension. A method to achieve this, is through composite action. It ensures the CFS section works primarily under tension while the concrete slab takes the compression by restricting the neutral axis in the concrete slab. Therefore, the composite action

facilities maximise the use of individual material properties.

Fig. 1. Local buckling in cold formed steel beam	**Fig. 2. Distortional bucking in cold formed steel beam**
Fig. 3. Lateral torsional buckling in cold formed steel beam [5]	
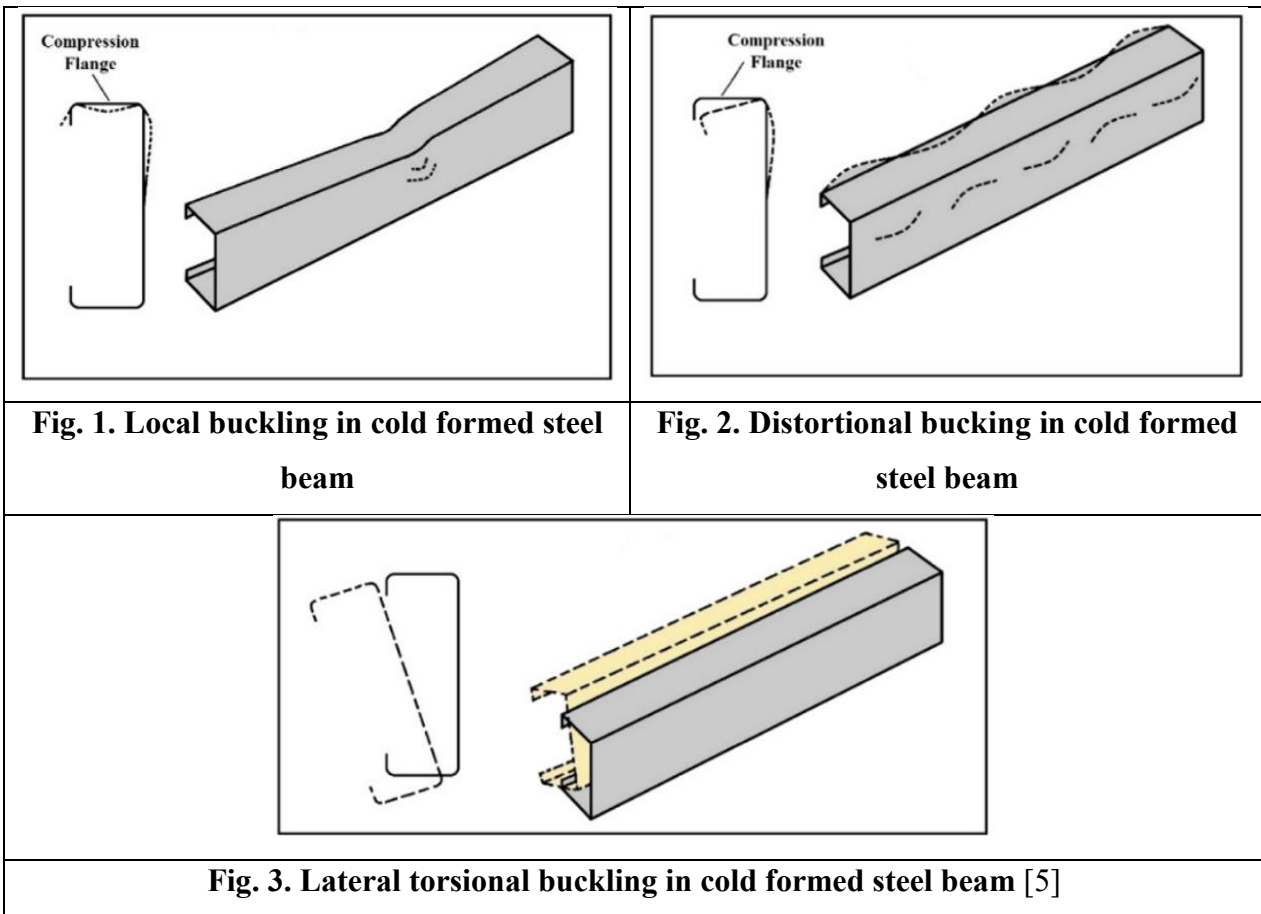
The attainment of full interaction is invariably dependent on the behavior of the shear connector. The shear connector is a mechanical device that transfers the longitudinal shear stresses at the interface of materials in composite elements [6]. Appropriate shear connectors are crucial for these systems' overall structural performance and integrity. Hence, significant research has been carried out over the years to investigate the performance of shear connectors in composite systems. Most of the shear connectors currently used in industries are studs, channels, and angle truss types, which are highly suitable for hot-rolled steel concrete composite construction [7]. These types of shear connectors are weldable, which cannot be adopted for light gauge cold-formed steel-concrete composite members. Since they are prone to geometrical deformation and residual stress formation under welding [9].

Thus, several researchers attempted to develop shear connectors of non-weldable types such as bolting, nailing [9], predrilled holes, bent-up taps [10], [11], embossments [12], bolted & screw connectors [7], [8], [13],[14], double channel, single channel connector and self-tapping screw shear connectors [15]. Predominantly, the available connectors for cold-formed steel concrete composite construction exhibit very low individual shear capacity and ductility. [16]–[18].
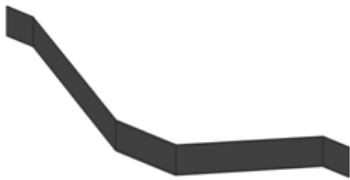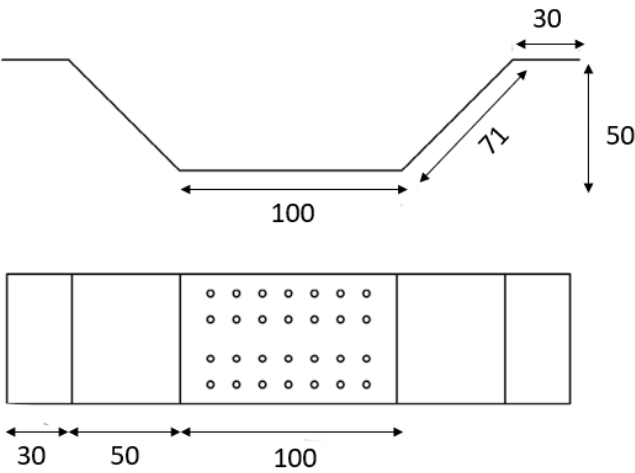
Thus, in this study attempts have been made to develop high capacity non weldable flexible shear connectors for cold-formed steel-concrete composite beams. Three novel connectors are proposed, and their performance was assessed based on their shear strength, slip modulus and ductility through push-out tests.

2. Proposed shear connectors.

The present study proposes three types of shear connectors suitable for cold-formed steel-concrete composite beams, namely trapezoidal, hexagonal, and prefabricated shear connectors (recently patented by the authors) [19]. These connectors were anchored on a double channel cold-formed steel beam connected back-to-back. The channel section was secured back-to-back by ten numbers of 16 mm diameter high friction grip bolts. For each variation three trail specimens were casted and tested.

2.1. Trapezoidal connector

The TC connector was fabricated by forging a steel sheet of 1.6 mm thick, and it consists of three parts: an anchoring zone, an inclined portion, and lips, as shown in **Figures 4. and 5.** The dimension of the TC specimen was 100 x 71 x 50 mm (anchorage zone x inclined portion x lips). The bearing area and weight of the connector were 7260 mm^2 and 0.170 kg, respectively. The anticipated capacity of the TC connector was calculated as 227 kN based on the yield strength and bearing area of the connector. Thus, twenty-eight self-drilling screws of 5 mm in diameter and 45 mm in length were drilled in the anchorage zone to secure a connector on either side of the flanges of the CFS beam, as shown in **Figure 5.** The inclined portions were provided to ensure effective stress transmission between the concrete and steel, whereas the lips were provided to arrest the upliftment stresses.

Fig. 4. Trapezoidal shear Connector	**Fig. 5.** Detailed drawing of trapezoidal shear connector

2.2. Hexagonal connector

The hexagonal connector was adopted with the idea of developing a composite shear connector rather than a steel connector. HC consists of a hexagonal steel pedestal, an anchorage zone and a concrete portion, as shown in **Figure 6.** The geometrical shape which occupies a higher cross-sectional area with a low circumference is the circle. The development of a circular-shaped shear connector showed fabrication difficulties; hence hexagonal shape was adopted for near-circular behaviour.

The hexagonal connector was fabricated by forging a 1.6 mm thick steel sheet. The anchorage zone of 25 mm in length was attached to the CFS beam, and the hexagonal pedestal zone of 50 mm in height, was embedded into the concrete. The pedestal zone, along with the confined concrete, was developed to act as a composite shear connector. The bearing area and weight of the HC connector were 3450 mm2 and 0.0974 kg, respectively. The anticipated capacity of the connector was 150 kN. Thus, eighteen self-drilling screws of 5 mm in diameter and 45 mm in length were drilled in the anchorage zone to secure a connector on either side of the flanges of the CFS beam, as shown in **Figure 7**. Both trapezoidal and hexagonal shear connectors are anchored on the beam by self-tapping screws of 3 mm diameter and 45 mm length.

Fig. 6. Hexagonal shear Connector	**Fig. 7.** Detailed drawing of hexagonal shear connector
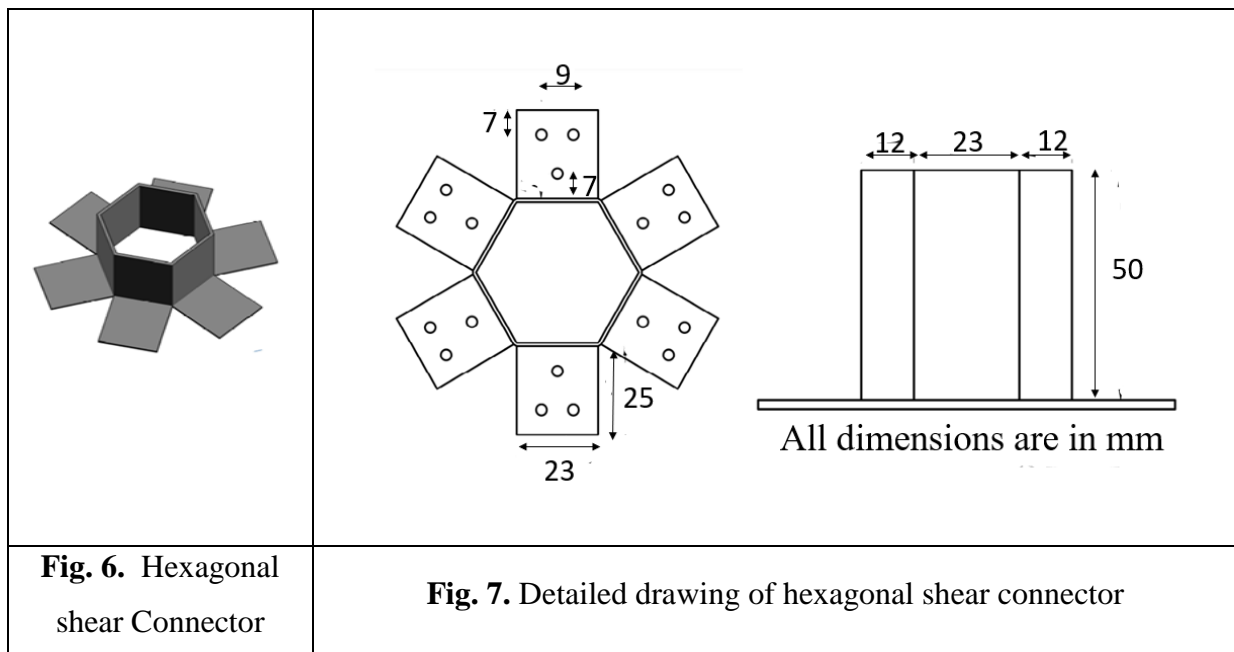
2.3. Prefabricated shear connector
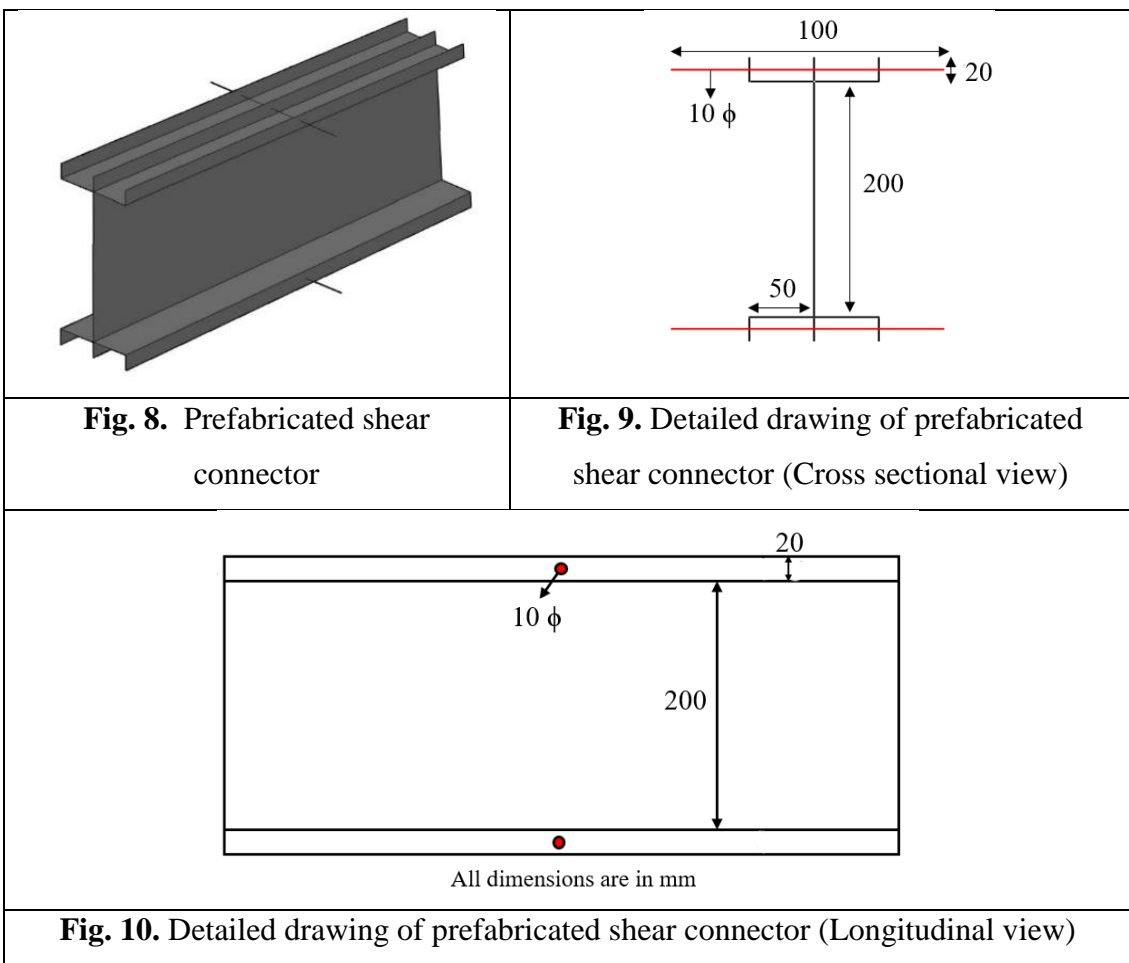
The prefabricated shear connector is a novel shear connector that can be easily adapted for cold-formed steel construction without welding, and the authors have recently patented it [19]. The prefabricated shear connector can be entirely formed in the fabrication yard. Usually, conventional shear connectors are installed on-site, which may disturb the speed of construction and shear connector

capacity. The prefabricated shear connector does not require any additional installation on-site, which makes it easier to install and less laborious.

In the prefabricated shear connector, the lips of the cold-formed double-channel beam were inverted, and a flat plate was inserted between the channels as shown in **Figure 8**. A reinforcement rod was made to pass through the inverted lips and the flat plate. The flat plate was provided throughout the length of the CFS beam to arrest the deformation of the rod while testing. This connector utilises part of the beam as a shear connector which may ensure a higher degree of composite action between the concrete slab and steel beam. The bearing area and weight of the connector were 2000 mm2 and 0.110 kg, respectively. **Figures 9 and 10.** illustrate the diagrammatic representation and detailed drawing of PF connector.

Fig. 8. Prefabricated shear connector	**Fig. 9.** Detailed drawing of prefabricated shear connector (Cross sectional view)

Fig. 10. Detailed drawing of prefabricated shear connector (Longitudinal view)

3. Material Properties

3.1 Material

A cold-formed steel channel section with a lip depth of 20 mm, flange width of 50 mm, web depth of 200 mm, thickness of 2.9 mm and length of 650 mm was employed in this study. These sections were connected back-to-back by bolts to form a double-channel cold-formed steel beam. The

trapezoidal and hexagonal shear connectors were extracted from steel sheets of 1.6 mm and formed. The longitudinal and transverse coupons were removed from steel sheets of both thicknesses (2.9 mm steel beam and 1.6 mm shear connector), as shown in **Figure 10**. They were tested as recommended in BS EN 10002-1[20], as shown in **Figure 11.** The yield strength, ultimate strength, modulus of elasticity and elongation percentage have been denoted as f_y, f_u, E, and y', respectively, as presented in **Table 1.**

The concrete was designed for the characteristic compressive strength of 30 MPa as per IS 10262-2019. The three trail cubes of 150 x 150 x 150 mm and three trail cylinders of 150 x 300 mm were cast and cured for 28 days. They were tested in accordance with IS 516-1959 [21]. The material properties of concrete are listed in **Table 2.**

Table 1 Material properties of coupon and reinforcing steel

Material	Dimension (mm)	f_y (MPa)	f_u (MPa)	y' (%)	E (MPa)
Tensile coupon	100 x 6 x 1.6	345	476	21.2	167000
	100 x 6 x 2.9	351	479	21.4	169000
Rebar rod	10 Ǿ	395	562	7.83	201012

Table 2 Material properties of concrete.

Properties	C1	C2	C3	Mean	σ	COV (%)
f_{cu} (MPa)	30.7	31.5	29.7	30.6	0.90	2.94
f_{cy} (MPa)	24.6	25.2	23.8	24.5	0.70	2.86
E_c (MPa)	27703.7	28062.4	27428.8	27658.6	317.7	1.15

3.2 Self-tapping Screws

A single-lap shear test was adopted to determine the shear capacity of the self-tapping screw. The tests were conducted on three different screw patterns. For each pattern, three specimens were adopted, and a total of nine specimens were fabricated and tested. The adopted patterns were single (S_a, S_b, S_c) and double nailed. In double nailed, two sets of arrangements were made, one is aligned parallel to the loading (PL_a, PL_b, PL_c), and the other is aligned perpendicular to the loading (PR_a, PR_b, PR_c).

The test setup consists of two steel plates of 300 mm in length, width of 70 mm and thickness of 1.6 mm connected with 5 mm self-tapping screws. These specimens were prepared in such a way that yielding of plates should not occur before the failure of connection. The tensile force was applied on plates with a UTM of capacity 100 tonnes. The applied tensile load will induce shear in the screws. The loading rate was kept at a constant rate of 0.5kN/min, and LVDTs connected to the DAQ system recorded the slip between the plates. The obtained data are presented in **Table 3.**

Table 3. Details of shear test of self-tapping screws

Specimen	S_a	S_b	S_c	PL_a	PL_b	PL_c	PR_a	PR_b	PR_c
L_c (mm)	45			45			45		
Φ (mm)	5			5			5		
C_c (kN)	2.95	2.93	2.91	5.9	5.78	5.82	5.89	5.84	5.74
C_{PS} (kN)	2.95	2.93	2.91	2.95	2.89	2.91	2.93	2.92	2.87
S_u (kN)	2.53	2.58	2.61	1.76	1.98	1.83	2.02	1.97	2.09

Fig. 10. Tensile Coupon Test Specimen

Fig. 11. Testing arrangement for the shear strength of self-tapping screws.
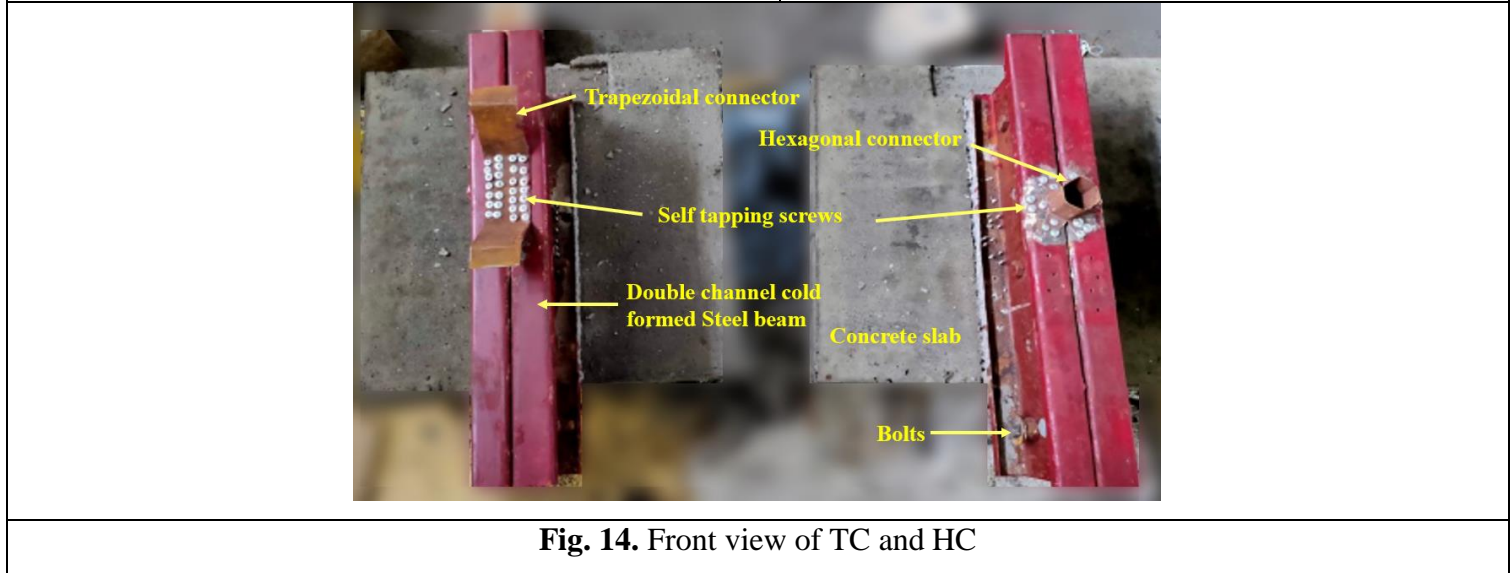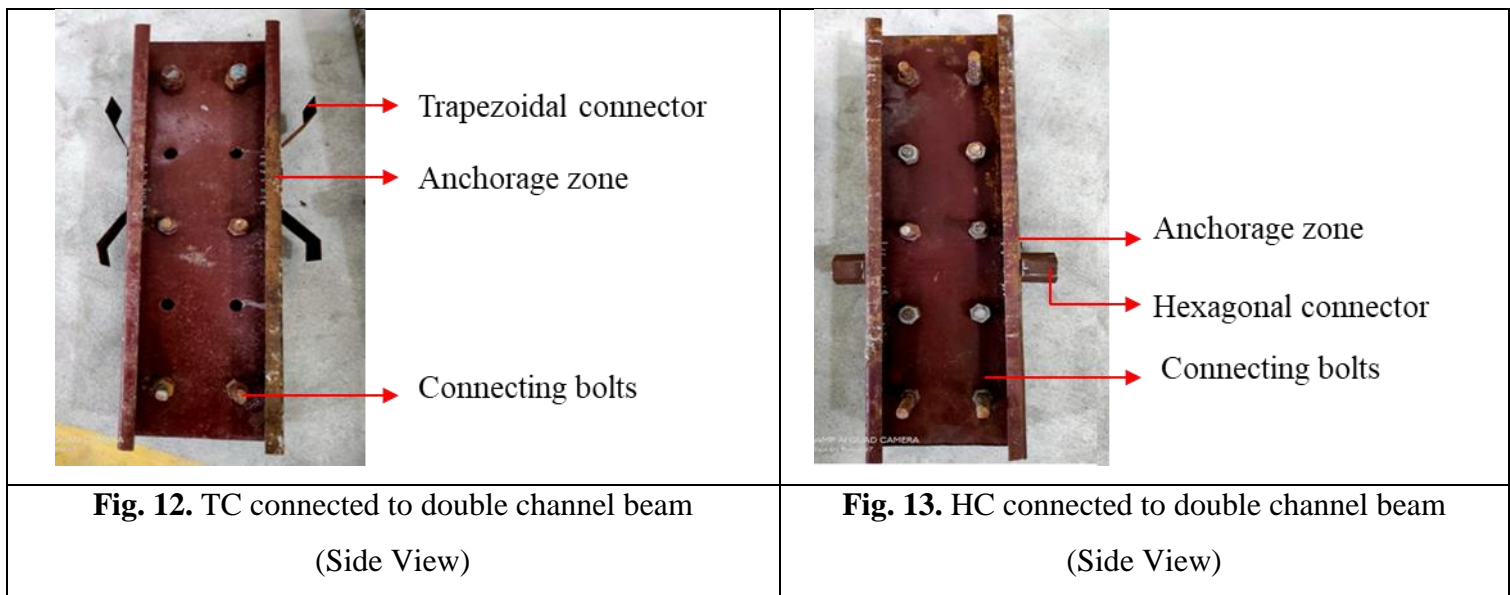
4. Experimental investigation

The conventional push-out test has been proven effective in studying the suitability of shear connectors in composite beams. It captures the ultimate strength, deformation, ductility, uplift, concrete cracking, and failure modes of the shear connector. Usually, in the push-out test set-up, two concrete slabs are cast on the flange of a steel I-beam on either side. The reinforcing rods are arranged in the perpendicular direction to the slab. The slab must be cast horizontally to reflect the actual construction practice.

In this study, the specimens were fabricated and cast as per the recommendations made in Eurocode 4 [22]. A double channel cold-formed steel beam connected back-to-back forms a core steel beam for a push-out test. The shear connectors are mounted on either side of the steel beam. The trapezoidal (**Figure 12**) and hexagonal (**Figure 13**) connectors are connected to the beam by self-tapping screws. Twenty-eight screws are used to connect the hexagonal connector, and eighteen screws for the trapezoidal connector.

The Prefabricated Shear Connector (**Figures 15 and 16**) utilizes a part of the steel beam as a shear connector. The lips were inverted in the core steel beam, and perforations were made to accommodate the reinforcement rods. The rods were inserted, and transverse reinforcement was laid over the

arrangement. The inverted lip portion and reinforcement rod were embedded in the concrete slab. This increases the bearing area of the concrete and enables easy transfer of stress between the components.

A total of nine specimens were prepared: three specimens for every connector. The nomenclature is adopted in alphanumerical style with an abbreviated alphabet mentioning the specimen's name followed by a numerical reference to the number of specimens. The trapezoidal, hexagonal, and prefabricated shear connectors were named HC, TC and PF. The specimens termed HC 1, whereas the first two letters indicate the type of connector, and the numerical value indicates the number of samples.
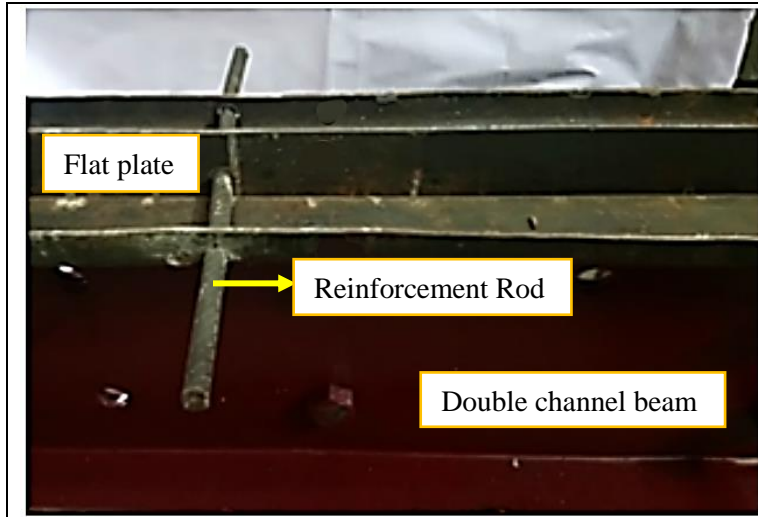
Fig. 12. TC connected to double channel beam (Side View)	**Fig. 13.** HC connected to double channel beam (Side View)

Fig. 14. Front view of TC and HC

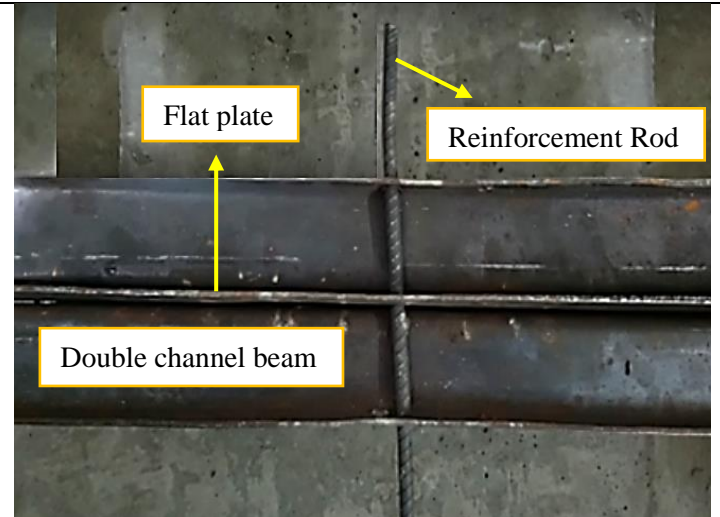|	
Fig. 15. Side view of PF connector	**Fig. 16.** Top view of PF connector

5. Push-out test loading protocol and instrumentation

The performance of the shear connectors was assessed by performing push-out test as per EC4. The specimen was placed on a solid 50 mm thick plate mounted over a strong floor. The loading was given with two hydraulic jacks of 300 kN capacity mounted on the loading frame. These jacks were connected to a solid I beam (spreader beam). This combined mechanism of the two jacks and an I-beam were coupled to give the specimen a maximum (600 kN) single-point load. A 20 mm thick plate was placed between the loading setup and the specimen to ensure proper load distribution.

An LVDT was placed to monitor the vertical displacement of the beam, and the load was observed by the load cell of 50 kN capacity. The integrity was monitored by the analogue system using a dial gauge and a proving ring. **Figures 17 and 18** illustrate the experimental setup and the schematic diagram of the test setup, respectively.

As per Eurocode 4, the load was cycled 25 times in the range of 5% to 40% of the expected failure load to ensure the equilibrium of the specimen. A constant loading rate of 5 kN per minute was maintained to ensure that none of the specimens failed before less than 15 minutes of testing. Three readings were recorded at every minute by the data acquisition system. The test was continued until the complete failure of the specimen.

Fig. 17. Push-out test setup	**Fig. 18.** Schematic diagram of push-out test arrangement of shear connector (HC)
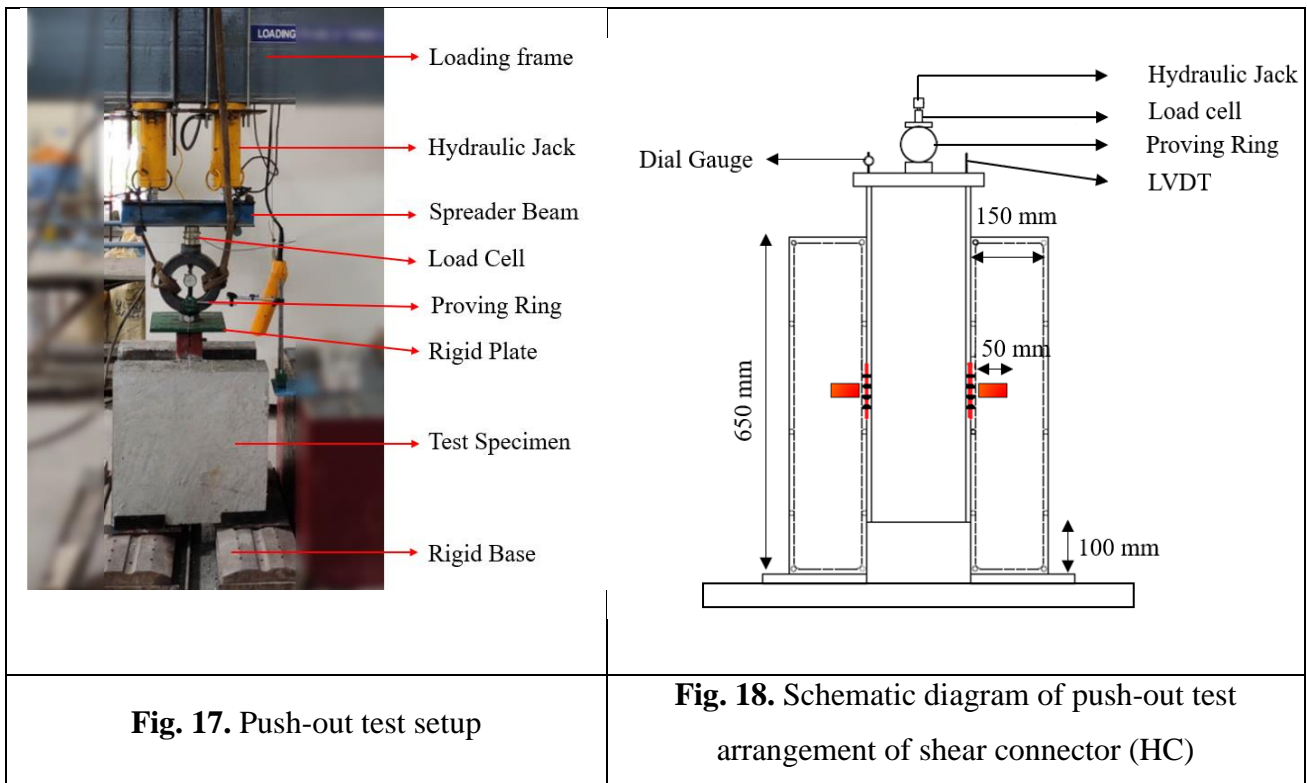
6. Results and Discussions

6.1 Failure mode

Rupturing of connector, crushing of concrete, and connection failure (failure of self-tapping screws) are the three possible failure modes in TC and HC connector.

1. Rupturing of connector:

   The rupture failure was initiated by the yielding of the connector, followed by tension failure at the reduced cross-section of the anchorage zone. The rupture failure was observed when the tension capacity of the shear connector was lesser than the bearing capacity of the concrete.

2. Crushing of concrete:

   The crushing failure was initiated by the cracking of concrete near the shear connector, followed by the complete crushing of concrete with mild deformation of the connector. This failure occurred when the bearing capacity of the concrete was lesser than the tension capacity of the connector. While testing, the thicker shear connector caused the crushing of near concrete when it tried to wimp out from the slab.

3. Connection failure:

   The connection failure was characterised by the shearing of anchorage self-drilling screws. This failure occurred when the load carrying of the shear connector was higher than the combined capacity of screws used in the anchorage zone.

11

6.2. Failure modes of shear connector:

The slim profile of the TC connector initiated the failure by rupture while the concrete remained undamaged. As the load increased, the connection failure was witnessed by shearing off the single-threaded self-drilling screws in the anchorage zone, as shown in **Figures 19 & 20**, whereas the lip portion prevented the connector from possible uplift and the inclined portion showed good bearing resistance.

Fig. 19. Failure of TC in Slab Portion	**Fig. 20.** Failure of TC in the Beam Portion

The HC connector adopted the technique of a composite shear connection system using the pedestal and the confined concrete in it. While loading, the connector experience shear at the anchorage zone and is transferred to the self-drilling screws, as shown in **Figures 21 and 22**. The applied forces generate tension on the upper side of the pedestal and in the self-drilling screws. The self-drilling screws experienced both shear and tension, which caused additional stress to the connection system, thus limiting the $HC_{1.6}$ connector's capacity by undergoing connection failure as shown in the **Figures 23 and 24**.

The PF connector was developed by adopting suitable modification in the cross-section of the beam without any anchoring mechanism. While testing, the PF connector failed due to the crushing of concrete around the connector and deformity of the rebar was detected, as shown in **Figures 25.**

1. The applied force.	3. The shear forces act on self-drilling screws.
2. The tension force in the pedestal.	4. Tensile force on screw.

Fig. 21. Forces on HC Connector	**Fig. 22.** Enlarged view of Connection System

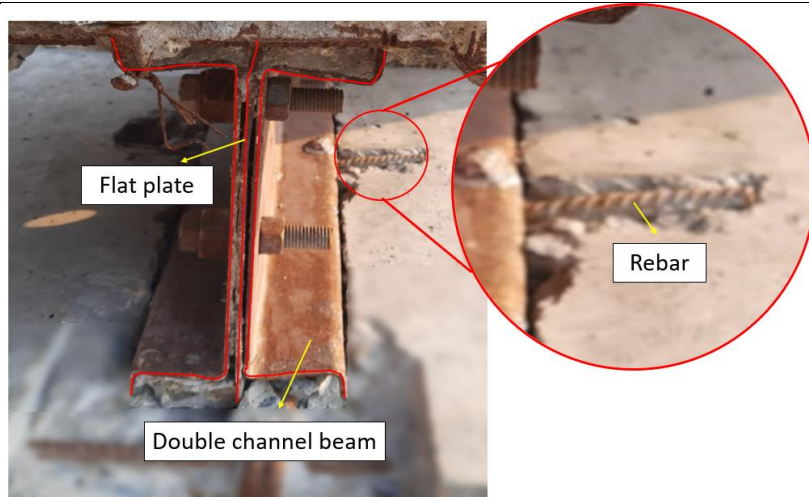| **Fig. 23.** Failure of HC in Slab Portion	**Fig. 24.** Connection Failure of HC in the Beam Portion

Fig. 25. Failure of PF in the Beam Portion

6.2 Mechanical characterisation

The typical load-slip curve of the pushout test with the salient points is shown in **Figure 26.** P_u is the ultimate load-carrying capacity of the connector, and P_{rk} is the characteristic resistance of the connector, divided by the number of connectors. P_{rk} is 0.9 times the ultimate load-carrying capacity of the connector (P_u). δ_u is the slip of the connector at the maximum value of P_{rk}. δ_{uk} is the characteristic slip capacity which is 0.9 times δ_u. The ultimate capacity, ultimate slip, and shear load capacity of all specimens are summarized in **Table 4.**
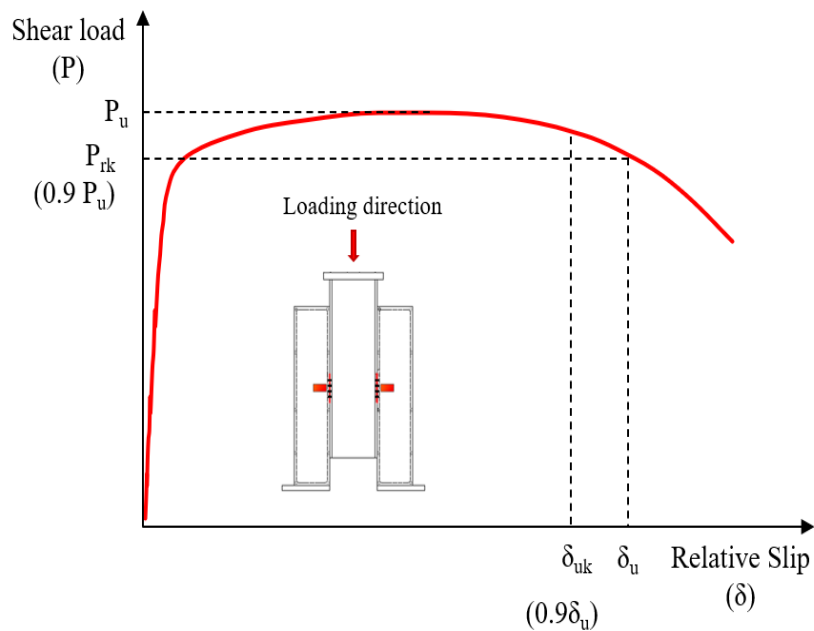

Fig. 26. Typical load-slip curve

6.3 Load slip curve

The average values of load-slip curves obtained from three identical specimens from each group were scrutinised and presented in **Table 4**

In TC connectors, the ultimate capacity (P_u) for the three trail specimens were recorded as 45.61, 46.12, and 44.9 kN at the ultimate slip (δ_u) of 4.5, 5.5, and 5.1 mm, respectively, as shown in **Figure 27.** The linear behaviour of the connector was observed up to 39 kN, and the initial stiffness was calculated as 48.56 N/m. Based on the equal area method, the average yield slip was calculated as 1.2 mm, and the corresponding average yield capacity was mapped as 43 kN. From the results, it is evident that the average yield slip was 41.70 % of the average ultimate slip.

In HC connectors, the ultimate capacity (P_u) for the three trail specimens were recorded as 52.82, 54.11, and 53.6 kN at the ultimate slip (δ_u) of 4.81, 5.01 and 5.43 mm, respectively, as shown in **Figure 28.** The linear behaviour of the connector was observed up to 35 kN, and the initial stiffness was calculated as 32 N/m. Based on the equal area method, the average yield slip was calculated as 1.2 mm, and the corresponding average yield capacity was mapped as 43 kN. From the results, it is evident that the yield slip (δ_y) was 23.80 % of the ultimate slip (δ_u).

In PF connectors, the ultimate capacity (P_u) for the three trail specimens were recorded as 153.5, 157.01, and 158.92 kN at the ultimate slip (δ_u) of 8.5, 6.9, and 7.1 mm, respectively, as shown in **Figure 29.** The linear behaviour of the connector was observed up to 123.46 kN, and the initial stiffness was calculated as 73 N/m. Based on the equal area method, the average yield slip was calculated as 1.96 mm, and the corresponding average yield capacity was mapped as 134.32 kN.

Figure 30 compares the average load slip curve of the proposed shear connector. The TC and HC connectors showed elastic and strain hardening zone. The PF connector exhibited elastic followed by strain hardening zone and strain softening zone.

The $\frac{P_u}{B_a}$ ratio (ultimate capacity to the bearing area of the connector) of all the connectors was calculated and tabulated in **Table 4**. This ratio depicts the maximum stress taken per mm^2 of the bearing area of the connector. The PF connector showed the highest $\frac{P_u}{B_a}$ ratio of 63.2 while the TC connector showed the least of 6.08, emphasising that the PF connector utilised the material to a greater extent than the TC connector. The PF connector outperformed other connectors with a 156 kN capacity and 8.0 mm slip. The PF showed remarkable individual shear capacity with good ductility.
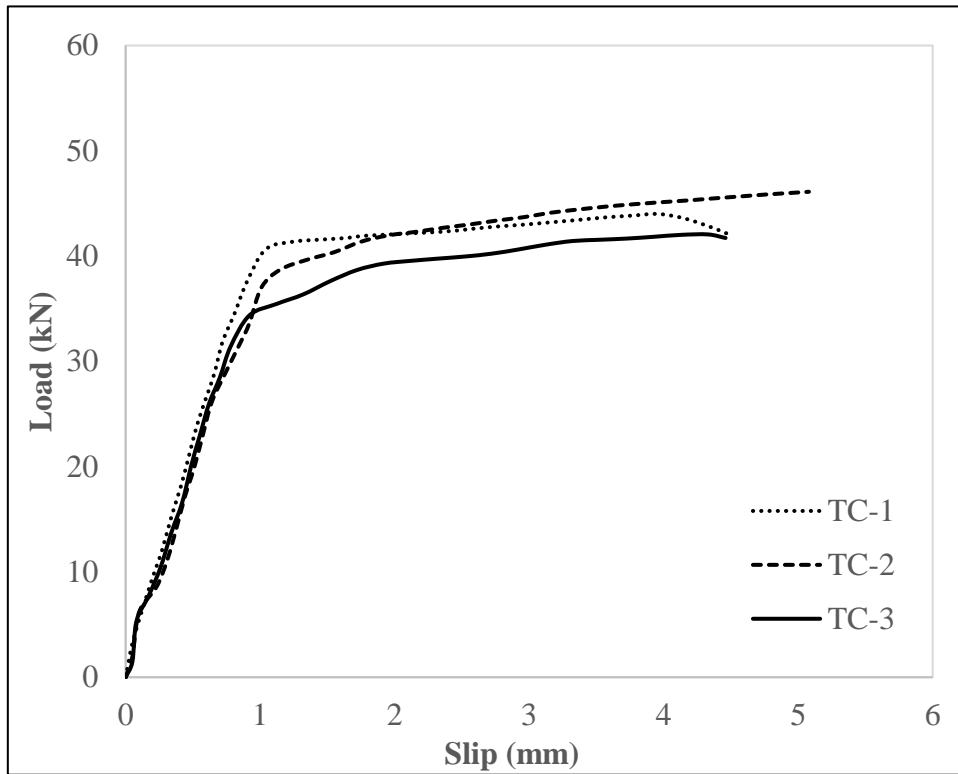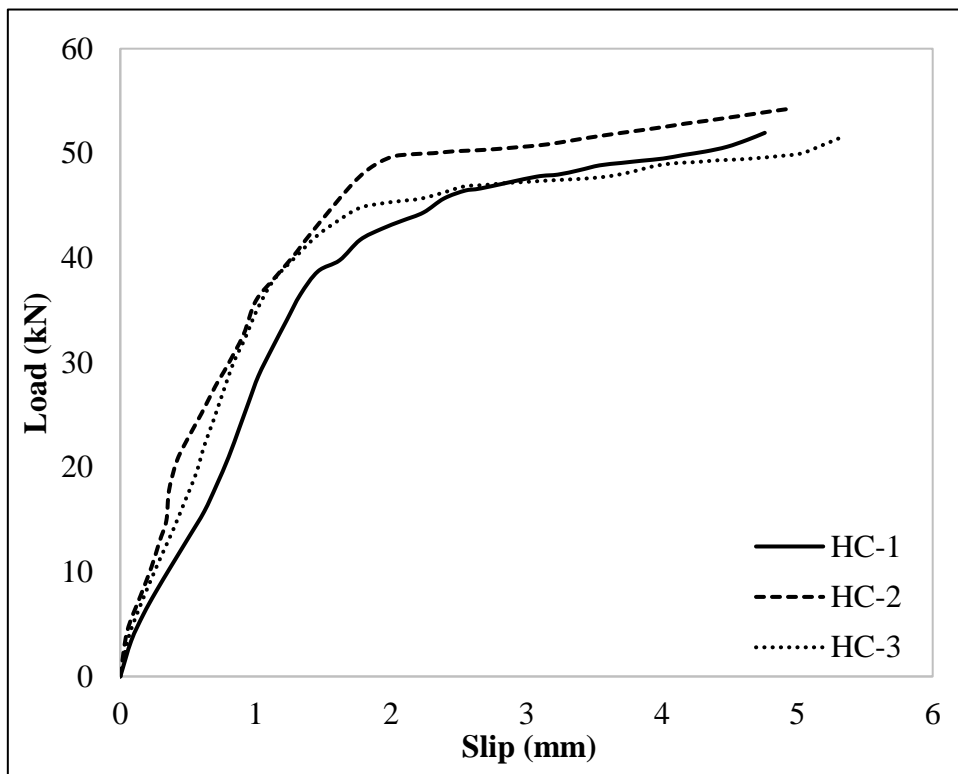
Fig. 27. Load vs. Slip of TC Specimens
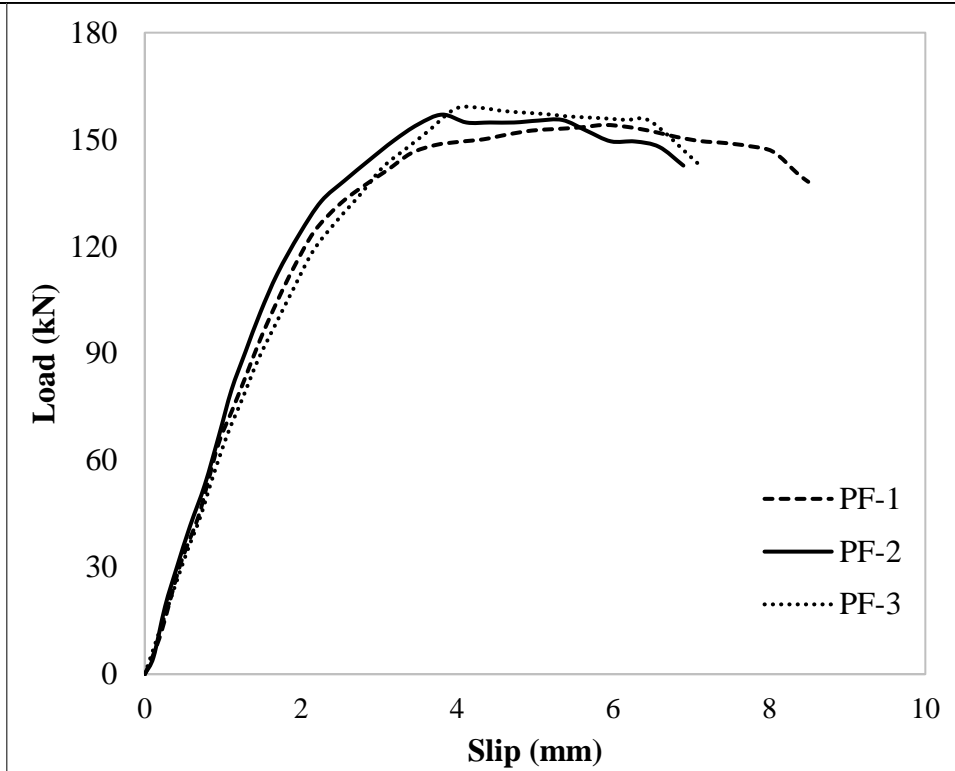

Fig. 28. Load vs. Slip of HC Specimens

16

Fig. 29. Load vs. Slip of PF Specimens
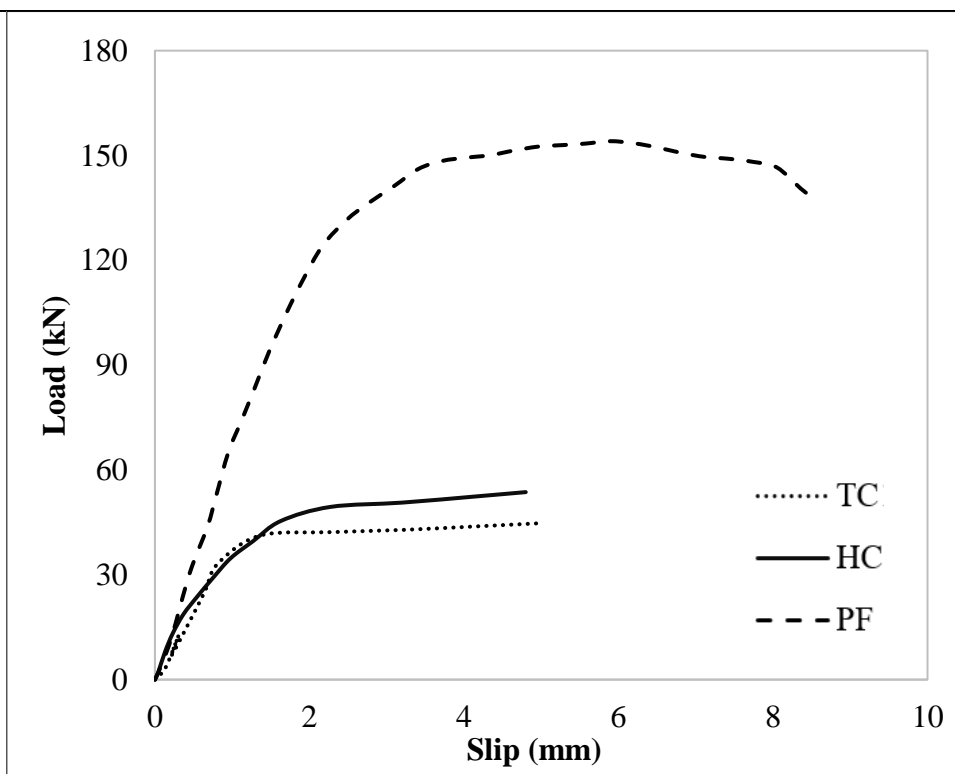
Fig. 30. The Average Load vs. Slip Curve of the Shear Connectors

17

Table 4 The comparison of P_u, P_{rk}, δ_u, δ_y.

Specimen		TC1	TC2	TC3	HC1	HC2	HC3	PF1	PF2	PF3
P_u (kN)		43.9	46.3	42.17	52.5	54.1	53.6	153.5	165.0	155.5
P_u avg (kN)			44.12			53.4			158	
P_{rk} (kN)		39.51	41.67	37.95	47.25	48.69	48.24	138.1	148.5	139.9
P_u	mean		44.9			53.4			158	
	σ		1.249			0.819			6.144	
	cov		2.782			1.533			3.889	
	β		1.61			3.00			1.47	
δ_u (mm)		4.5	5.5	5.1	4.81	5.01	5.43	8.5	6.9	7.1
δ_{uk} (mm)		4.1	5.0	4.6	4.3	4.5	4.9	7.7	6.2	6.4
δ_y (mm)		1.39	1.37	1.36	1.09	1.12	1.11	2.2	1.98	1.99
δ_u/δ_y avg (DF)			3.67			4.59			3.7	
B_a (mm^2)			7260			3450			2500	
$\dfrac{P_u}{B_a}$			6.08			15.48			63.2	

6.5 Ductility analysis

The ductility of the connector enables the redistribution of stresses in structural elements before any noticeable failure occurs [23]. The load slip behavior of the proposed connectors is shown in the **Figure 31**. The evaluation of ductility of the connector through load–slip behavior is by introducing an equivalent bilinear curve, as illustrated in **Figure 32**. Two types of the bilinear curve were generated to simulate the behavior of the shear connector. One is elastic linear hardening, and the other is an elastoplastic curve. The load slip curve of TC and HC specimens showed an elastic and significant strain hardening zone. Hence, it was idealized as an elastic hardening curve. Whereas the PF connector showed an elastic and negligible hardening zone. Thus, it was idealized as an elastoplastic curve.

From the idealized bilinear curve, yield displacement (δ_y) was calculated based on the equal area method. According to Eurocode, the ultimate slip (δ_u) is taken beyond the ultimate load carrying capacity, which corresponds to the maximum value of P_{rk}. The equivalent ductility factor (DF) is taken as the ratio of ultimate slip to yield slip (δ_u/ δ_y). The DF of each specimen was calculated and presented in **Table 4**. As presented in **Table 4**, the HC connector showed the least yield slip (δ_y) of 1.09 mm, followed by the TC specimen at 1.39 mm. The PF connector also recorded the highest yield slip of 2.2 mm, which reflected the same trend in ultimate slip.
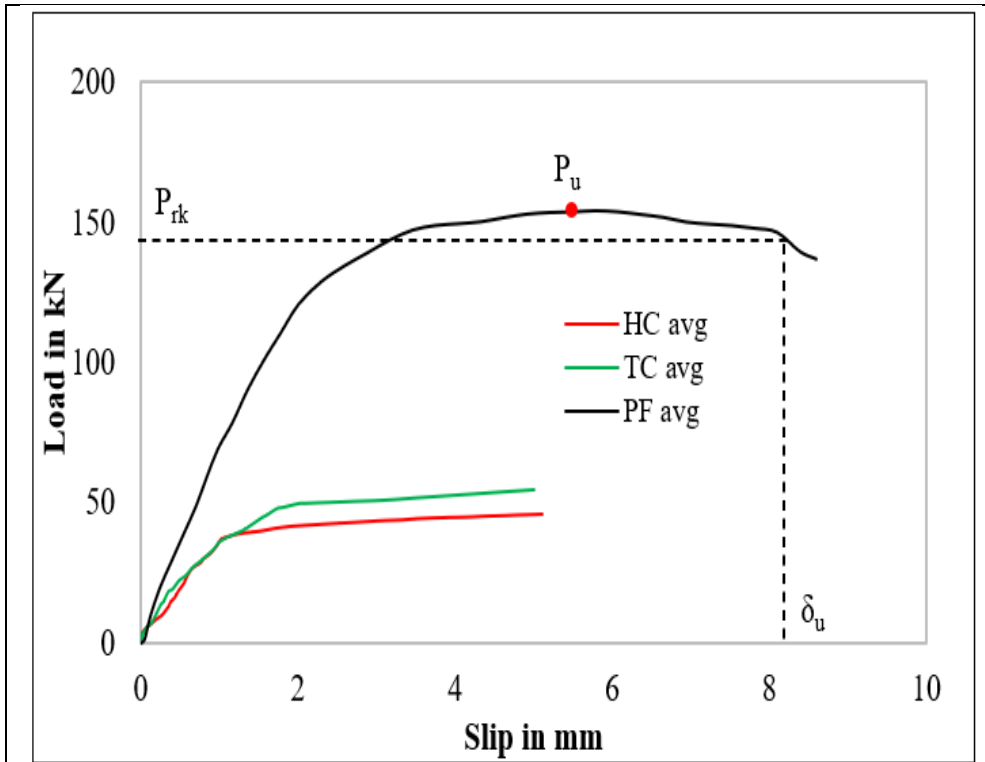
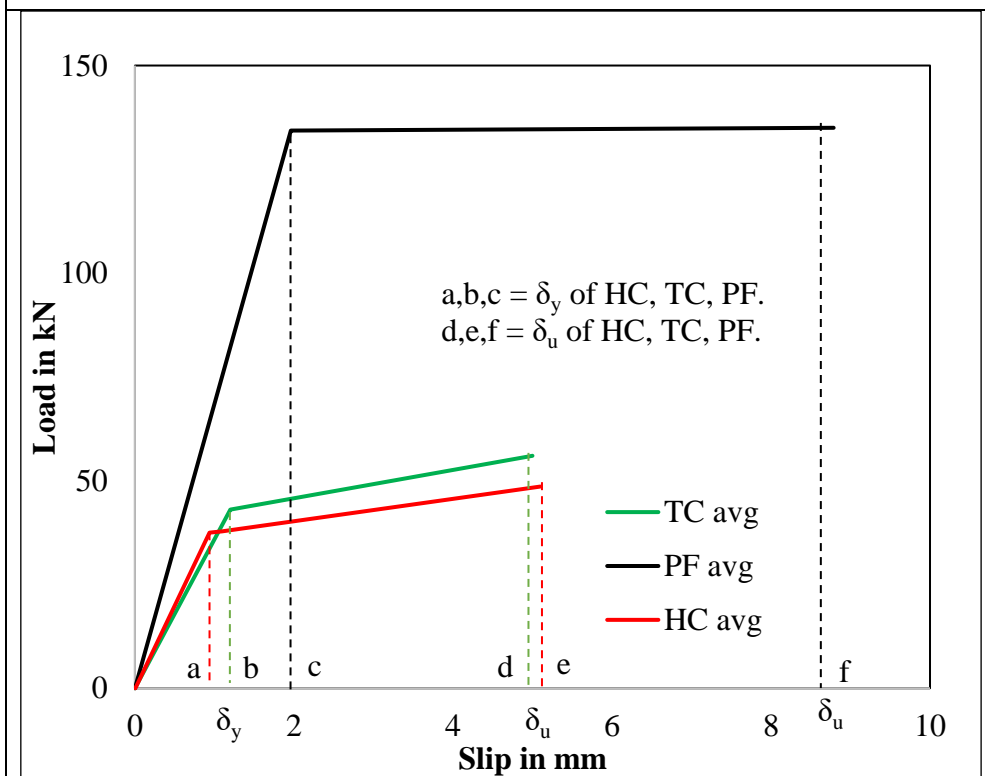**Fig. 31.** Average load vs. slip curve of HC, TC and PF connector

Fig. 32. Idealized average load vs. slip curve of HC, TC and PF connector

19

7. Energy absorption capacity (EA)

An effective method to estimate the load-carrying capacity of a structural element is the energy concept. The structure should possess the energy absorption or the dissipation mechanism to counteract the excessive loading. Usually, the elements tend to undergo irreversible energy conversion to dissipate the developed kinetic energy. Such conversion is feasible when an element has a good energy-absorbing capacity.

The energy absorption capacity can be estimated by calculating the area under the average load slip curve of the tested specimens, presented in **Figure 33**. The area was calculated using the trapezoidal rule by taking an equal interval of 0.1 mm slip. The load slip curve of TC and HC connectors shows relatively lesser slip for average ultimate capacity than PF connectors. The energy absorption capacity of the connector is directly dependent on the area under the load slip curve.

From **Figure 34**, it is highly evident that the PF connector showed the highest average energy absorbing capacity of 1,165.95 joules, while HC and TC specimens showed 202.06, and 227.44 joules. The energy absorption capacity of the PF connector is nearly 5.7 times more than HC and TC connectors. From the results, it can be concluded that the PF connector can absorb higher energy than the other connectors.

Fig. 33. Definition of energy absorption factor by load-slip curve	**Fig. 34.** Average energy absorption capacity of shear connectors
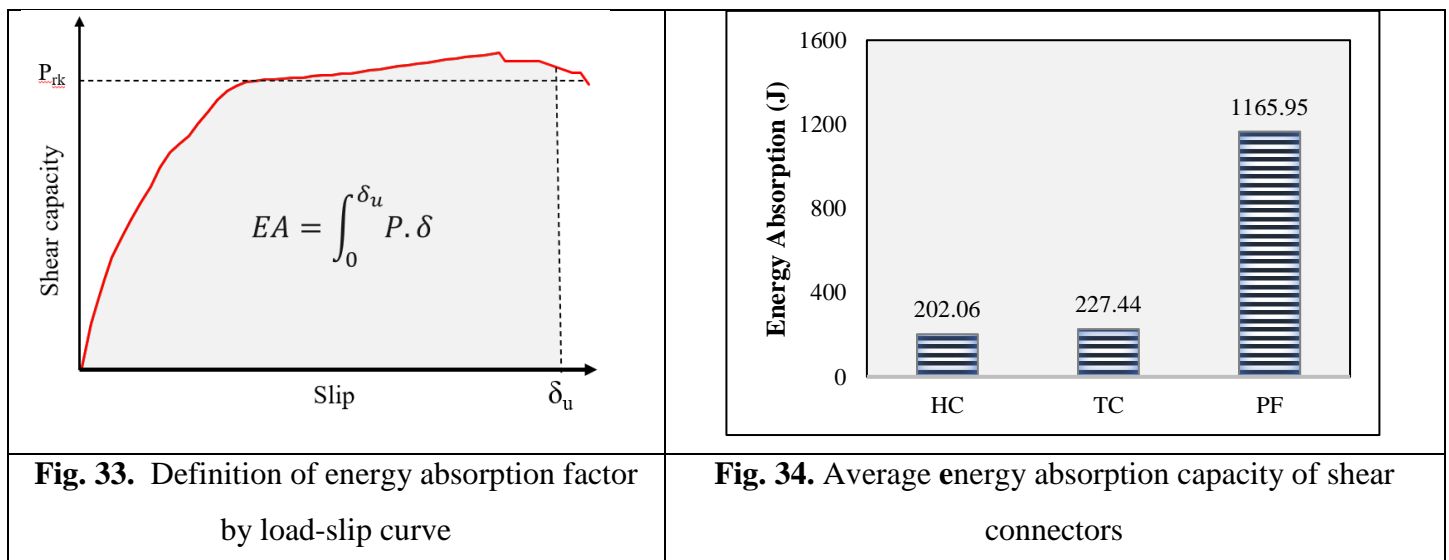
8. Reliability Analysis

Based on the codal guidelines of NAS-2016, the relative reliability of the pushout test was calculated from the equation 1. The parameters in the equations 1 of reliability index (β) were derived from statical analysis. The values were calculated as 1.10. 1.00, 0.10 and 0.05 for M_m, F_m, V_m and V_f respectively while the value M_m, F_m, P_m, V_m and V_f are the mean value for material, fabrication factor, professional factor, coefficient of variation and correction factor for number of trail specimens adopted

for each variation. For load and resistance factor design, the coefficient of variation of load effect V_Q and calibration coefficient C_φ was taken as 0.21 and 1.52 respectively. The three-pushout tests were done for every variation and correction factor (C_p) was taken as 5.7 and the resistance factor (φ) based on NAS-2016 and IS 800 respectively.

$$\beta = \frac{\ln\left(\frac{M_m F_m P_m C_\varphi}{\phi}\right)}{\sqrt{V_P^2 + V_M^2 + V_F^2 + V_Q^2}} \tag{1}$$

The target reliability index was taken as 3.0. Most of the test results indicated higher reliability with reliability index more than 3.0.

9. Proposed Cold-formed Connectors vs. Hot-rolled Connectors.

Table 5 compares the specifications of the conventional hot rolled stud connector, channel connector and the proposed cold-formed shear connectors. The details of stud and channel connectors were considered as recommended in IS 11384-1985. The yield stress of the stud and channel connector as listed in IS 11384 as 540 and 250 MPa respectively. The yield stress of HC, TC and PF connectors were 160, 168 and 415 MPa respectively. The weight of HC and TC connectors along with the anchoring zone was 0.195 and 0.340 kg. The weight of rebar in the prefabricated shear connector was 0.110 kg. The ultimate capacity of HC, TC and PF connectors were 95 kN, 66.98 kN, and 158 kN respectively. The proposed HC, TC and PF connector has the strength to weight ratio of 490, 190 and 1436 however the conventional stud and channel connector have the strength to weight ratio of 262 and 140 respectively. The proposed cold-formed shear connector exhibited superior performance to the hot-rolled connectors. From the experimental results, it was found that PF and HC connector has a fivefold and a threefold increase in the strength-to-weight ratio than the conventional hot rolled shear connectors, respectively.

From the above discussion, it is evident that the PF connector outperforms all the proposed connectors with high individual shear capacity, better performance, and good adaptability with out any anchoring system.

Table 5
Comparison of HC, TC and stud connectors

Connectors	Dimension (dia*length) mm	Thickness (mm)	W_c (kg)	Grade of concrete	P_u (kN)	$\frac{P_u}{W_c}$
STC1	25 x100	-	0.385	M30	101*	262

CH1	125*65*150	5.3	1.57	M30	219^	140
HC	-	1.6	0.195	M30	95.6	490
TC	-	1.6	0.340	M30	66.98	197
PF	10 x 200	10 (rod)	0.110 (rod)	M30	158.0	1436

9. CONCLUDING REMARKS

In this study, nine pushout tests were carried out to investigate the performance of TC, HC and PF connectors. The shear capacity, shear stiffness, ultimate slip and load-slip relationship of these three connectors were examined and compared with existing hot-rolled and cold-formed connectors. The following are the observations from the analysis of the results:

1. Three non-weldable cold formed shear connectors such as trapezoidal, hexagonal, and prefabricated shear connectors are proposed to be an alternative for weldable connectors.

2. The HC specimens behaves like a composite pedestal. Hence, it experienced a 20% higher capacity than TC specimens, while its cross-sectional area accounts for only 70% of TC specimens. Thereby, conforming that confining effect is also a crucial parameter in determining the shear capacity of the connector.

3. The PF connector showed three times higher shear capacity with two times higher slip capacity than TC and HC specimens. The PF connector also showed higher initial stiffness and longer plastic phase than other connectors.

4. The PF connector recorded a maximum of 1,162.5 joules of energy absorbing capacity, while TC and HC specimens accounted for 227.4 and 202.1 joules, respectively which shows its suitability to be used as an effective shear connector.

5. TC and HC specimens showed the behavior of non-ductile connectors with low characteristic slip capacity. Thus, they can be used only for full interaction composite beams. But the PF connector behaves ductile, which can also be adopted for partial interaction beams.

6. The PF connector is highly economical and easy for mass production. It does not require any sophisticated equipment for fabrication and installation.

10. REFERENCES

[1]   G. J. Hancock, "Cold-formed steel structures," *J. Constr. Steel Res.*, vol. 59, no. 4, pp. 473–487, 2003, doi: 10.1016/S0143-974X(02)00103-7.

[2]   G. Mulligan and T. Pekoz, "Locally Buckled Thin-Walled Columns," *J. Struct. Eng.*, vol. 110, no. 11, pp. 2635–2654, 1984, doi: doi:10.1061/(ASCE)0733-9445(1984)110:11(2635).

[3]   W. K. Kenneth, M. ASCE, G. Winter, and F. ASCE, "Effects of Cold-forming on Light-gage

Steel Members," *J. Struct. Div. Proc. Am. Soc. Civ. Eng.*, vol. 93, no. 1, pp. 433–469, 1967.

[4]   C. Yu and B. W. Schafer, "Local Buckling Tests on Cold-Formed Steel Beams," *J. Struct. Eng.*, vol. 129, no. 12, pp. 1596–1606, 2003, doi: 10.1061/(ASCE)0733-9445(2003)129:12(1596).

[5]   E. Hosseinpour, S. Baharom, W. H. Wan, and A. W. Al Zand, "Push-out test on the web opening shear connector for a slim-floor steel beam: Experimental and analytical study," *Eng. Struct.*, vol. 163, pp. 137–152, May 2018, doi: 10.1016/j.engstruct.2018.02.047.

[6]   D. Lam and E. El-Lobody, "Behavior of Headed Stud Shear Connectors in Composite Beam," *J. Struct. Eng.*, vol. 131, no. 1, pp. 96–107, 2005, doi: 10.1061/(ASCE)0733-9445(2005)131:1(96).

[7]   A. Hanaor, "Tests of composite beams with cold-formed sections," *J. Constr. Steel Res.*, vol. 54, no. 2, pp. 245–264, 2000, doi: 10.1016/S0143-974X(99)00046-2.

[8]   A. Saggaff *et al.*, "Experimental and Analytical Study of Various Shear Connectors Used for Cold-Formed Steel-Ferrocement Composite Beam," *Appl. Mech. Mater.*, vol. 754–755, pp. 315–319, 2015, doi: 10.4028/www.scientific.net/amm.754-755.315.

[9]   P. Kyvelou, L. Gardner, and D. A. Nethercot, "Composite Action Between Cold-Formed Steel Beams and Wood-Based Floorboards," *Int. J. Struct. Stab. Dyn.*, vol. 15, no. 08, p. 1540029, 2015, doi: 10.1142/S0219455415400295.

[10]   B. S. Lakkavalli and Y. Liu, "Experimental study of composite cold-formed steel C-section floor joists," *J. Constr. Steel Res.*, vol. 62, no. 10, pp. 995–1006, 2006, doi: 10.1016/j.jcsr.2006.02.003.

[11]   J. M.Irwan, A. H. Hanizah, and I. Azmi, "Test of shear transfer enhancement in symmetric cold-formed steel-concrete composite beams," *J. Constr. Steel Res.*, vol. 65, no. 12, pp. 2087–2098, 2009, doi: 10.1016/j.jcsr.2009.07.008.

[12]   B. R. P. Nguyen, "Thin walled cold-formed steel composite beams," vol. 117, no. 10, pp. 2936–2952, 1992.

[13]   N. Wehbe, P. Bahmani, and A. Wehbe, "Behavior of Concrete/Cold Formed Steel Composite Beams: Experimental Development of a Novel Structural System," *Int. J. Concr. Struct. Mater.*, vol. 7, no. 1, pp. 51–59, 2013, doi: 10.1007/s40069-013-0031-6.

[14]   T. M. Alhajri *et al.*, "Behavior of pre-cast U-Shaped Composite Beam integrating cold-formed steel with ferro-cement slab," *Thin-Walled Struct.*, vol. 102, pp. 18–29, 2016, doi: 10.1016/j.tws.2016.01.014.

[15]   S. Rajendran, J. Perumalsamy, and D. Mohanraj, "Push out tests on various shear connectors used for cold - formed steel composite beam," *Steel Compos. Struct.*, vol. 3, pp. 315–323,

2022.

[16] M. Paknahad, M. Shariati, Y. Sedghi, M. Bazzaz, and M. Khorami, "Shear capacity equation for channel shear connectors in steel-concrete composite beams," *Steel Compos. Struct.*, vol. 28, no. 4, pp. 483–494, 2018, doi: 10.12989/scs.2018.28.4.483.

[17] K. Nouri, N. H. R. Sulong, Z. Ibrahim, and M. Shariati, "Behaviour of novel stiffened angle shear connectors at ambient and elevated temperatures," *Adv. Steel Constr.*, vol. 17, no. 1, pp. 28–38, 2021, doi: 10.18057/IJASC.2021.17.1.4.

[18] M. Shariati *et al.*, "A novel approach to predict shear strength of tilted angle connectors using artificial intelligence techniques," *Eng. Comput.*, vol. 37, no. 3, pp. 2089–2109, 2021, doi: 10.1007/s00366-019-00930-x.

[19] D. R. Senthilkumar, M. Divya, D. P. Jayabalan, and D. B. A, "Cold-formed steel-concrete composite beam with a prefabricated shear connector and method thereof" Indian patent no: 414619. Granted on 15.12.2022.

[20] *EN B. 10002-1: 2001. Tensile testing of metallic materials. Method of test at ambient temperature.* British Standards Institution., 2001.

[21] *IS 516 (1959): Method of Tests for Strength of Concrete.* New Delhi: Bureau of Indian Standards, 1959.

[22] E. 1994-1-1, *EUROCODE 4: Design of composite steel and concrete structures - part 1-1: general rules and reules for building*, vol. 1. 2004.

[23] S. Gao, Q. Bai, L. Guo, S. B. Kang, A. Derlatka, and S. Deng, "Study on flexural behavior of spliced shallow composite beams with different shear connectors," *Eng. Struct.*, vol. 253, no. January, p. 113816, 2022, doi: 10.1016/j.engstruct.2021.113816.